PHYSICAL REVIEW C **78**, 021601(R) (2008)

Dipole polarizability of ^{7}Li from precision measurement of the elastic scattering on ^{208}Pb below the Coulomb barrier

V. V. Parkar,* V. Jha,† B. J. Roy, S. Santra, K. Ramachandran, A. Shrivastava, A. Chatterjee, S. R. Jain, A. K. Jain, and S. Kailas
Nuclear Physics Division, Bhabha Atomic Research Centre, Mumbai 400 085, India
(Received 31 March 2008; published 27 August 2008)

The effect of dipole polarizability (α_0) of ^{7}Li due to its cluster structure has been determined from a high precision elastic scattering measurement of ^{7}Li on ^{208}Pb, over a range of energies from $E_{\rm lab} = 18$–28 MeV($V_{\rm Coul} \approx 30$ MeV). Continuum discretized coupled channel (CDCC) calculations have been performed to describe the measured elastic scattering data.

DOI: 10.1103/PhysRevC.78.021601 PACS number(s): 25.70.Bc, 24.10.Eq, 21.60.Gx, 25.70.De

Nucleus-nucleus elastic scattering at energies well below the Coulomb barrier is influenced by the polarizability of the light projectile, induced by the strong Coulomb field of the heavy target nucleus [1]. The interaction of the induced dipole moment of the projectile with the electric field $E(R)$ generated by the target, leads to a polarization potential which, in the adiabatic limit, is given as [2]

$$V_{\rm pol}(R) = -\frac{1}{2}\alpha_0 E(R)^2 = -\frac{1}{2}\alpha_0 \frac{Z_T^2 e^2}{r^4}, \qquad (1)$$

where α_0 is the dipole polarizability, $Z_T e$ is the charge of the target nucleus, and r is the separation between the center of masses of the projectile and target. As a result, the effective Coulomb potential ($V_{\rm eff} = Z_P Z_T e^2/r + V_{\rm pol}$) gets reduced and the effect shows up as a small but measurable deviation (reduction) from pure Rutherford scattering in the elastic scattering of the projectile from the target.

Careful measurements have been carried out to determine the α_0 values for d [3] and ^{3}He [4] from highly accurate elastic scattering data of these projectiles from ^{208}Pb target. In the case of weakly bound stable projectiles like ^{6,7}Li, ^{9}Be and light radioactive nuclei, due to the low break-up threshold, the Coulomb field is expected to alter the elastic scattering in the following ways: (i) the strong Coulomb field will lead to breakup of the weakly bound projectiles, resulting in a loss of flux and the consequent reduction in the elastic scattering process; (ii) the projectile will be polarized due to the Coulomb field and this will lead to a decrease in the elastic scattering cross section. For stable projectiles, the dipole strength is usually located at fairly high excitation energies and hence coupling of the ground state (g.s.) to the dipole states is not significant. However, due to low break-up threshold for the weakly bound projectiles, substantial dipole strength could be energetically possible at the lower excitation energies for these nuclei [5]. This, in turn, will favour a strong dipole coupling between the ground state and states in the continuum lying above the break-up threshold. The polarizability of the projectile is related to the dipole distribution $B(E1)$ as [6]

$$\alpha_0 = \frac{8\pi}{9}\sum_{n\neq 0}\frac{B(E1; gs \rightarrow n)}{\epsilon_n} \qquad (2)$$

where ϵ_n is the energy of the nth dipole state.

It is possible to treat all these aspects in case of weakly bound projectiles in terms of a complex polarization potential, where the real term of the polarization potential will take care of the polarizability effect and the associated imaginary part will account for loss of flux due to absorption. The above features are also amenable to CDCC calculations so that one could attempt a consistent description of not only the elastic but also the inelastic and fusion channels. It may be remarked that the coupling to low lying continuum for a weakly bound projectile may lead to both attractive and repulsive contributions depending on the bombarding energies. This feature will have a bearing on the final behavior of the elastic scattering cross section. The CDCC formalism has been applied successfully to describe the elastic scattering data involving ^{6}He [7] and ^{7}Li [8]. In particular, the absence of a characteristic Coulomb rainbow and a strong reduction in elastic cross section for ^{6}He + ^{208}Pb system has been attributed to the couplings due to dipole excitations [7]. Attempts have been made to deduce the value of α_0 for ^{7}Li from analyses of elastic and inelastic scattering of ^{7}Li from ^{208}Pb [8,9]. We have carried out high precision cross section measurements for this system, reducing the systematic and statistical uncertainties. We have analyzed the present data set combining it with related inelastic (excitation of ^{7}Li) and fusion data within the framework of the CDCC formalism assuming α-t cluster model for ^{7}Li nucleus. The contribution to the value of α_0 due to the coupling of the low-lying break-up states and its effect on elastic scattering cross section has been calculated.

We have made a theoretical estimate of the polarizability α_0 of ^{7}Li within the α-t cluster model. The dipole moment is induced by a perturbative potential $V_{\rm pert}$, which is given as

$$V_{\rm pert} = -\frac{2}{7}\frac{Z_T e^2}{R^3}(\vec{r}\cdot\vec{R}), \qquad (3)$$

where $\vec{r}$ is the relative displacement between clusters, $\vec{R}$ is the center of mass coordinate, and θ is the angle between them. The polarizability is expressed in terms of second-order Stark effect due to this potential in the presence of the electric field

*vvparkar@barc.gov.in
†vjha@barc.gov.in

arising from the target:

$$\alpha_0 = \frac{8}{49}\left(\frac{2m_{\alpha t}}{\hbar^2 c^2}\right)\sum_{n\neq 0}\frac{\langle 0|ez|n\rangle\langle n|ez|0\rangle}{{k_n}^2+\gamma^2}. \quad (4)$$

Here $z = r\cos\theta$, $m_{\alpha t}$ is the reduced mass of the α-t cluster, and quantities k_n and γ are defined as ${k_n}^2 = \frac{2m_{\alpha t}E_n}{\hbar^2}$, $\gamma^2 = \frac{2m_{\alpha t}\epsilon}{\hbar^2}$ with $\epsilon = -E_{\alpha t} = 2.47$ MeV being the separation energy of the α-t cluster. Employing the Green function approach, and using the cluster wave function [10,11], an analytic calculation of α_0 yields an estimate [12] of about 0.02 fm^3.

The experimental measurements reported here were performed using the ^{7}Li beam (intensity ~40–80 enA) from the 14UD BARC-TIFR pelletron accelerator, Mumbai. The beam was defined by two circular collimators of diameter 2 mm and 3 mm located at 50 cm and 60 cm, respectively, upstream of the target. The target was enriched ^{208}Pb (>98%) of thickness ≈175 μg/cm^2. The isotopic composition of Pb material was confirmed from a mass analysis using the Inductively Coupled Plasma Mass Spectrometer (ICP-MS) of Vacuum Physics and Instrumentation Division (VPID), Bhabha Atomic Research Centre (BARC), Mumbai. The ^{208}Pb was evaporated on carbon backing with a backing thickness of about 40 μg/cm^2. The events corresponding to scattering from carbon were expected to be kinematically well separated from the events of interest. An elemental analysis (using the XRF facility of Nuclear Physics Division (NPD), BARC) of the target was also performed to bring out the presence of trace level impurities with mass numbers close to ^{208}Pb. The detectors used were Si surface barrier in ΔE (25–30 μm)-E (500–1000 μm) telescope configuration. Two such identical telescopes were placed symmetrically to the left and right of the incident beam at ±40° and ±160° (Fig. 1) to eliminate, in the first order, the effect due to possible beam wandering and consequent changes in scattering. The angular resolution of the detectors was 0.2° and 0.7° for forward and backward telescopes, respectively. The angle offsets of the movable arms on which the detectors had been placed, were measured by a theodolite. The counting rate dead time variations between different telescopes were corrected by acquiring the events from pulsers for each detector and by counting them directly using scalars. A consistency check was done by repeating the measurements at some of the energy points. The entire measurement, apart from the angular distribution measurement which was done toward the end of the experiment, was performed without any alteration of the setup or moving the detectors in anyway. Data at all energy points were accumulated for sufficiently high statistics to reach a statistical uncertainty of about 0.4%, the best so far for this system. For each energy, the data was taken for nearly 4–6 h and it was divided into 8–12 intervals of about 30 min each to check the consistency and then added to get higher statistics. Careful analysis of the elastic peak region was carried out to determine the elastic cross section reliably devoid of small uncertainties due to nearby 0.48 MeV excited state of ^{7}Li. In addition to the measurement of the ratio of elastic cross sections at fixed angles, angular distribution data were also collected at $E_{\rm lab} = 27$ MeV with the same set of detector telescopes.

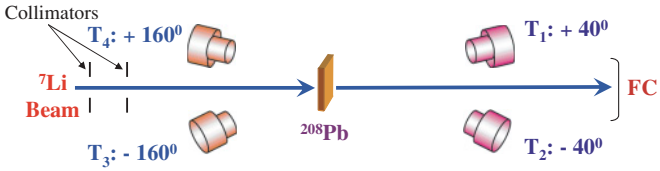

FIG. 1. (Color online) Schematic illustration of experimental setup for the precise measurement of elastic scattering in ^{7}Li + ^{208}Pb reaction.

To calculate the deviation of elastic data from Rutherford scattering at backward angle as a function of energy we define the ratio $R(E)$ following Ref. [3] as

$$R(E) = \frac{\sqrt{C_L\left(E_{\rm ref},\theta_L^F\right)\cdot C_R\left(E_{\rm ref},\theta_R^F\right)}}{\sqrt{C_L\left(E_{\rm ref},\theta_L^B\right)\cdot C_R\left(E_{\rm ref},\theta_R^B\right)}} \times \frac{\sqrt{C_L\left(E,\theta_L^B\right)\cdot C_R\left(E,\theta_R^B\right)}}{\sqrt{C_L\left(E,\theta_L^F\right)\cdot C_R\left(E,\theta_R^F\right)}}, \quad (5)$$

where C_L, C_R are the number of counts recorded in the detectors kept at angles $\theta_L^{F(B)}$ and $\theta_R^{F(B)}$ for the two energies $E_{\rm ref}$ and E (the subscripts L, R refer to telescopes kept at left and right of the beam direction, respectively, while the superscripts F, B refer to forward and backward telescopes, respectively). In the present experiment, $\theta_{L(R)}^F = 40°$ and $\theta_{L(R)}^B = 160°$ and $E_{\rm ref} < E$ (with $E_{\rm ref} = 18$ MeV which is well below the Coulomb barrier and $E = 18$–28 MeV). The above ratio is free from uncertainties due to beam wandering, detector solid angle and the target thickness. The overall error on the data points for ratio $R(E)$ was assigned to be ~0.4–0.5%; due to statistics.

A good charge and mass resolution was achieved which allowed the separation of ^{7}Li from other particles (Fig. 2). The energy resolution [ΔE(FWHM) = 150 keV for the forward telescopes and 230 keV for the backward telescopes] was sufficient to resolve the elastic peak from the inelastic excitation of ^{7}Li($\frac{1}{2}^-$, $E_x = 0.48$ MeV). Also the events corresponding to scattering from the carbon backing were well separated as shown in the inset of Fig. 2.

The double ratio $R(E)$ extracted from the measured elastic scattering data (counts) is shown in Fig. 3 along with the calculations (cross sections) which are described later. The result shows a gradual reduction with respect to the Rutherford cross section which is visible from the energy $E_{\rm lab} = 23$ MeV. The low energy cross sections measured here can be influenced by other effects, e.g., atomic screening, relativistic correction and vacuum polarization apart from the dipole polarizability effects. However, these effects are expected to be small [1] and almost angle independent and therefore contribute very little to the ratio value. The noninclusion of these effects will lead a systematic error of $\lesssim$0.2%; in the estimation of $R(E)$ [3,4,13]. The measured elastic scattering angular distribution data at 27 MeV are shown in Fig. 4. These data have relatively larger errors (typically ~1%; for forward angles and ~2%; for backward angles).

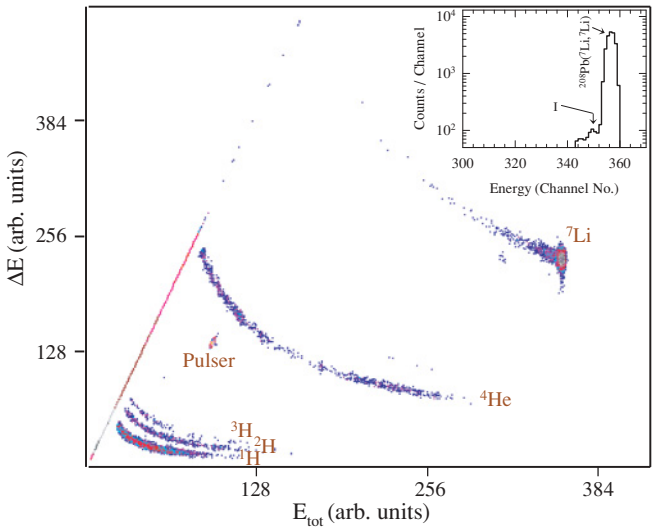

FIG. 2. (Color online) A typical two dimensional spectrum of ΔE vs. $E_{\rm tot}$ for ^{7}Li + ^{208}Pb measured at $E_{\rm lab} = 27$ MeV and $\theta_{\rm lab} = 160^\circ$. The inset shows the projected spectrum of ^{7}Li band onto the x-axis. The arrow (labeled as 'I') indicates the expected position of ^{7}Li inelastic excitation ($\frac{1}{2}^-$, 0.48 MeV) state.

In order to understand the observed dependence of the ratio $R(E)$, and to extract the value of dipole polarizability, a detailed CDCC calculation was performed. While the elastic scattering at energies much above the Coulomb barrier is dominated by nuclear effects, the data at lower energies is strongly influenced by the Coulomb force. To determine the value of α_0 reliably, it is important to fix the nuclear potential and the contributions from the inelastic couplings. The available data at higher energies have been used to determine the nuclear part of the interaction. In addition to elastics, the inelastic scattering data and the fusion data for

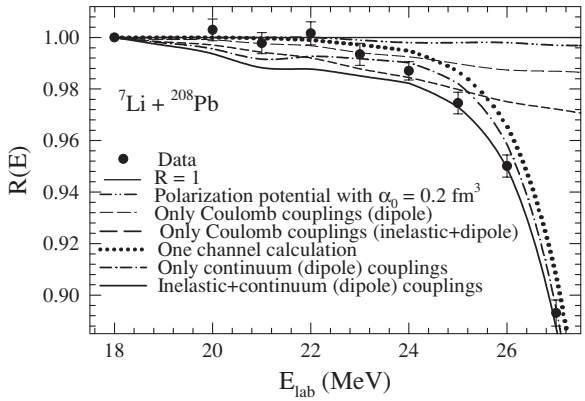

FIG. 3. Measured ratio, $R(E)$, of the elastic scattering cross section with $R(E)$ as defined in the text. The curves represent the CDCC calculations with bare nuclear potential + g.s. reorientation (dotted line), including the dipole couplings (dot-dashed line), additional inelastic coupling to ^{7}Li ($\frac{1}{2}^-$, 0.48 MeV) state (solid line). The short dashed and medium dashed lines shows the CDCC calculations with couplings due to Coulomb part only. The dot-dot-dashed line is obtained by calculations using a polarization potential with $\alpha_0 =$ 0.2 fm^3 as defined in Eq. (1).

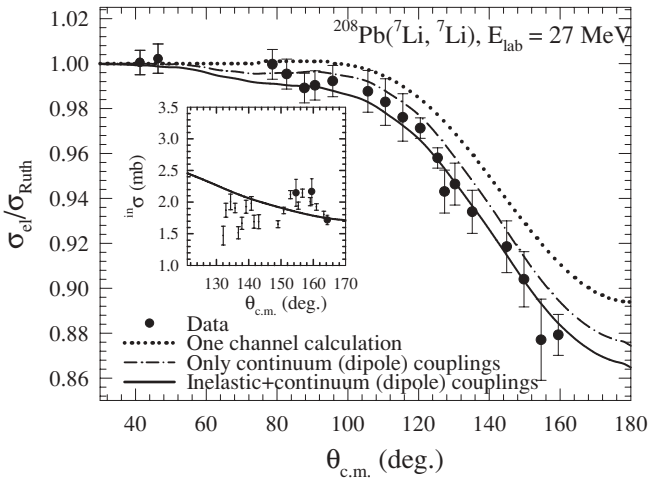

FIG. 4. Measured ratio $\sigma_{\rm el}/\sigma_R$ of elastic scattering cross section for the system ^{7}Li + ^{208}Pb as a function of c.m. scattering angle. The curves are the CDCC calculations with bare nuclear potential + g.s. reorientation (dotted line), including the dipole couplings (dot-dashed line) and additional inelastic coupling to ^{7}Li ($\frac{1}{2}^-$, 0.48 MeV) state (solid line). Inset shows the inelastic data (the filled circles are from the present measurements while the other data is taken from Ref. [8]) and the comparison with CDCC calculations (solid line).

^{7}Li + ^{209}Bi were used to constrain various parameters. The CDCC calculations were carried out by means of the computer code FRESCO (version frxy.li) [14]. The calculations assumed a two body α-t cluster picture for the ^{7}Li nucleus. The ground state and inelastic excitation of ^{7}Li were considered as pure $L = 1$ cluster states, where L is the relative angular momentum of clusters. The continuum above the ^{7}Li $\rightarrow \alpha + t$ break-up threshold was discretized into momentum bins of constant width $\triangle k = 0.25\,{\rm fm}^{-1}$, where $\hbar k$ is the momentum of α-t relative motion. The binding potential for all the cluster bound and continuum states were taken from the literature [15]. The cluster wave functions for each bin in the continuum were averaged over the bin width and the resulting wave function was normalized to unity. In the CDCC approach, each of these bins is then treated as an excited state of ^{7}Li with excitation energy equal to mean of the bin energy range. In the present set of calculations, the scattering wave functions were integrated up to 200 fm with the step of 0.05 fm and up to 350 partial waves were used.

The calculations require α-^{208}Pb (V_α) and t-^{208}Pb (V_t) optical model potentials at 4/7 and 3/7 of the incident ^{7}Li energy, respectively, for the calculations of the diagonal and coupling potentials using the cluster-folding method. As stated earlier, a determination of accurate input potentials is imperative for a proper account of nuclear effects. These potentials were derived and validated in a systematic way by fitting the available elastic scattering and fusion data at higher energies from the literature. The available global set of potentials for α-^{208}Pb [16] and for t-^{208}Pb [17] were first used for the description of high energy elastic scattering data [18] by a full CDCC calculations taking into account all the continuum bins ($L = 0$, 1, 2, and 3). The real part for both the potentials were normalized by a factor 0.6 for obtaining a good fit

to the experimental data. This normalisation was necessary specially for the correct description of the Fresnel diffraction bump observed in the higher energy data of Ref. [18]. Due to the low energies involved in the present case, which are below the energy regions for which these potentials are strictly valid, an additional energy-dependent normalisation factor was obtained for the imaginary part. This was obtained by fitting the existing data of elastic and fusion cross section at higher energies simultaneously, which was subsequently extrapolated to the energy of interest. Since the fusion cross sections for ^{7}Li + ^{208}Pb were not available in the literature, these were taken from the nearby system ^{7}Li + ^{209}Bi [19]. The fusion cross sections were obtained in CDCC calculations by the one dimensional barrier penetration model with the help of effective potential consisting of a bare cluster-folded potential and the polarization potential generated by all continuum couplings. After fixing the bare nuclear potentials, we proceed with the calculations at lower energies (E < 28 MeV) for studying the effect of dipole polarizability. The potentials used in the calculation are listed in Table I.

In earlier calculations [8] for $E_{\rm lab} = 27$ MeV, it was observed that the most important effect in the elastic and inelastic channel was due to the couplings to the $L = 0$ continuum bins placed at relatively lower excitation energies above the break-up threshold. This is indeed the case even for elastic scattering at lower energies that has been measured in the present experiment. Additional couplings due to the $L = 0$ bins placed at higher energy as well as the $L = 2$ bins were found not to significantly alter the calculated elastic scattering cross section at lower energies. Further the $L = 1, 3$ continuum bins were found to affect the elastic and inelastic channels very little at lower energies while they have the dominant contribution at the beam energy of 33 MeV [20] and at higher energies. An important observation is that the coupling to the continuum is found to have an opposite effect on the elastic scattering differential cross section for the energies below and above the Coulomb barrier. At lower energies the cross sections are reduced by the coupling to the continuum (due to the importance of dipole polarization couplings, $L = 1$ g.s. $\rightleftharpoons L = 0$ continuum) while at higher energies they are increased (due to the couplings of $L = 1$ g.s. $\rightleftharpoons L = 1, 3$ continuum). Thus, it is implied that the total polarization potential associated with the dipole transitions is attractive while it is repulsive for the transitions to the continuum having same parities as that of the ground state.

The results of the calculations for the ratio $R(E)$ and for elastic angular distribution at 27 MeV are compared to the experimental data in Figs. 3 and 4, respectively. The calculations have taken into account the possible ^{7}Li inelastic excitation ($\frac{1}{2}^{-}$, 0.48 MeV) and couplings due to ground state reorientation. The latter, though having a significant effect at higher energies, is found to be considerably weaker at energies below the Coulomb barrier. The dotted line of Figs. 3 and 4 shows the calculations with the bare potential along with the ground state reorientation while the dot-dashed line represents the calculations where the dipole coupling effects (only due to cluster with $\alpha_0 \sim 0.045$ fm^3) have been taken into account. Due to the relatively large value of $B(E2)$ (6.80 e^2 fm^4), inelastic coupling of ^{7}Li bound inelastic excitation ($\frac{1}{2}^{-}$, 0.48 MeV) has a significant contribution to the elastic scattering cross sections. The final calculations shown by the solid line in Figs. 3 and 4 takes into account the effect of all dipole couplings together with the inelastic couplings of ^{7}Li. The inclusion of coupling to the break-up states (dot-dashed line), and coupling to the ^{7}Li inelastic ($\frac{1}{2}^{-}$, 0.48 MeV) state (solid and dotted lines) tend to reduce the elastic cross sections. This is consistent with the effect of an attractive polarization potential, as obtained by the couplings of inelastic and dipole transitions. Calculations were also performed to estimate the effect of target inelastic excitations and were found to be quite insignificant (less than 0.2% at the highest energy of 28 MeV). Therefore, all the effects of variation of elastic scattering cross sections at lower energies can be safely ascribed to projectile inelastic excitation and the dipole couplings. It may be remarked that the measured inelastic scattering ($\frac{1}{2}^{-}$, 0.48 MeV) data for few angles at 27 MeV and those reported in Ref. [8] are well explained by the calculations as shown in inset of Fig. 4. The fusion data for ^{7}Li + ^{209}Bi [19] are also consistent with the present calculations. We have also investigated the continuum couplings effect due to Coulomb part only by comparing it with total coupling effects. As is shown by dashed line of Fig. 3, Coulomb couplings are the dominating factor in lower energy region while at higher energies nuclear couplings take over.

As mentioned in Ref. [8] dipole polarizability of ^{7}Li can have significant contribution also from the n-^{6}Li and p-^{6}He single particle states. However, dipole strength due to these states are concentrated at relatively higher excitation energies and are expected to affect the elastic cross section less as compared to cluster states which are located at low

TABLE I. Potential parameters used in CDCC calculations. The geometrical parameters are as follows: For $\alpha + ^{208}$Pb, $r_R = 1.25$ fm, $a_R = 0.77$ fm, $r_I = 1.57$ fm, $a_I = 0.57$ fm, $r_C = 1.50$ fm; For $t + ^{208}$Pb, $r_R = 1.20$ fm, $a_R = 0.72$ fm, $r_I = 1.40$ fm, $a_I = 0.84$ fm, $r_C = 1.30$ fm, where $R_x = r_x(A_T^{1/3})$, $x = R$ or I. Note: The calculations are insensitive to the imaginary depth below $E_{\rm lab} =$ 24 MeV.

System	$E_{\rm lab}$[MeV]	18	19	20	21	22	23	24	25	26	27
$\alpha + ^{208}$Pb	V_0[MeV]	109.4	109.3	109.2	109.1	109.0	108.9	108.9	108.8	108.7	108.6
	W_0 [MeV]	0.0	0.0	0.0	0.0	0.0	0.0	0.5	0.5	1.1	1.7
$t + ^{208}$Pb	V_0 [MeV]	97.4	97.4	97.3	97.3	97.2	97.2	97.1	97.1	97.1	97.0
	W_0 [MeV]	0.0	0.0	0.0	0.0	0.0	0.0	1.9	1.9	3.8	5.7

excitation energies. A simplified calculation using Eq. (1) for the polarization potential has been performed with a value of $\alpha_0 = 0.2\,\mathrm{fm}^3$ as deduced from the photo-absorption measurement data. The calculation predicts a very small reduction in the value of ratio $R(E)$ as shown in Fig. 3 (dot-dot-dashed line) in contrast to measurable deviation in $R(E)$ values predicted by a more accurate CDCC calculation which included only pure dipole couplings (Fig. 3, medium dashed line).

In summary, we have reported the measurements of highly precise elastic scattering cross sections [ratio $R(E)$ with an overall uncertainty of 0.4–0.5%] over a range of energies, from sub-barrier to near barrier. While we have demonstrated sensitivity to dipole strength (α_0 due to cluster part) in the CDCC calculation of $R(E)$ values, a reliable experimental determination of α_0 from the present high precision data is not feasible due to the "systematic errors" in the calculation arising from competing inelastic excitation (first excited state of ^{7}Li) and sensitivity to nuclear potential at higher energies.

The authors would like to thank the operation staff of the Pelletron Accelerator for providing high quality beam during the experiment. The help during the experiments from P. Shukla, U. K. Pal, and A. B. Parui is gratefully acknowledged. We thank the Forschungszentrum Juelich for providing enriched ^{208}Pb material and the target laboratory, TIFR for making the targets. Thanks are due to the mass separator laboratory of VPID, BARC for isotopic analysis and to the XRF laboratory of NPD, BARC for impurity scan of the target. We would like to acknowledge the suggestions from Prof. K. Rusek and Prof. I. J. Thompson which helped in improving the calculations.

[1] G. Baur, F. Rosel, and D. Trautmann, Nucl. Phys. **A288**, 113 (1977).
[2] N. F. Ramsey, B. J. Malenka, and U. E. Kruse, Phys. Rev. **91**, 1162 (1953).
[3] N. L. Rodning, L. D. Knutson, W. G. Lynch, and M. B. Tsang, Phys. Rev. Lett. **49**, 909 (1982).
[4] F. Goeckner, L. O. Lamm, and L. D. Knutson, Phys. Rev. C **43**, 66 (1991).
[5] M. V. Andrés and J. Gómez-Camacho, Phys. Rev. Lett. **82**, 1387 (1999).
[6] R. A. Broglia and A. Winther, *Heavy-Ion Reactions* (Part I FIP Lecture Notes Series) (Addison-Wesley, New York, 1991).
[7] K. Rusek, N. Keeley, K. W. Kemper, and R. Raabe, Phys. Rev. C **67**, 041604 (2003).
[8] I. Martel, J. Gómez-Camacho, K. Rusek, and G. Tungate, Nucl. Phys. **A641**, 188 (1998).
[9] O. Hausser, A. B. McDonald, T. K. Alexander, A. J. Ferguson, and R. E. Warner, Phys. Lett. **B38**, 75 (1972).
[10] Y. C. Tang, K. Wildermuth, and L. D. Pearlstein, Phys. Rev. **123**, 548 (1961).
[11] A. K. Jain and N. Sarma, Nucl. Phys. **A195**, 566 (1972).
[12] S. R. Jain, A. K. Jain, and S. Kailas, preprint.
[13] W. G. Lynch, M. B. Tsang, H. C. Bhang, J. G. Cramer, and R. J. Puigh, Phys. Rev. Lett. **48**, 979 (1982).
[14] I. J. Thompson, Comput. Phys. Rep. **7**, 167 (1988).
[15] B. Buck and A. C. Merchant, J. Phys. G **14**, L211 (1988).
[16] V. Avrigeanu, P. E. Hodgson, and M. Avrigeanu, Phys. Rev. C **49**, 2136 (1994).
[17] C. M. Perey and F. G. Perey, At. Data Nucl. Data Tables **17**, 1 (1976).
[18] I. Martel, J. Gómez-Camacho, K. Rusek, and G. Tungate, Nucl. Phys. **A605**, 417 (1996).
[19] M. Dasgupta, D. J. Hinde, K. Hagino, S. B. Moraes, P. R. S. Gomes, R. M. Anjos, R. D. Butt, A. C. Berriman, N. Carlin, C. R. Morton *et al.*, Phys. Rev. C **66**, 041602(R) (2002).
[20] K. Rusek, J. Gómez-Camacho, I. Martel-Bravo, and G. Tungate, Nucl. Phys. **A614**, 112 (1997).